

rf magnetron sputter deposition of transparent conducting Nb-doped TiO₂ films on SrTiO₃

Meagen A. Gillispie, Maikel F. van Hest, Matthew S. Dabney, John D. Perkins, and David S. Ginley

Citation: *J. Appl. Phys.* **101**, 033125 (2007); doi: 10.1063/1.2434005

View online: <http://dx.doi.org/10.1063/1.2434005>

View Table of Contents: <http://jap.aip.org/resource/1/JAPIAU/v101/i3>

Published by the [American Institute of Physics](#).

Related Articles

Epitaxial growth of Ti₃SiC₂ thin films with basal planes parallel or orthogonal to the surface on α -SiC
Appl. Phys. Lett. **101**, 021606 (2012)

Room-temperature remote-plasma sputtering of c-axis oriented zinc oxide thin films
J. Appl. Phys. **112**, 014907 (2012)

Ion mass spectrometry investigations of the discharge during reactive high power pulsed and direct current magnetron sputtering of carbon in Ar and Ar/N₂
J. Appl. Phys. **112**, 013305 (2012)

Visible light emission and energy transfer processes in Sm-doped nitride films
J. Appl. Phys. **111**, 123105 (2012)

Shape control of nickel nanostructures incorporated in amorphous carbon films: From globular nanoparticles toward aligned nanowires
J. Appl. Phys. **111**, 114309 (2012)

Additional information on *J. Appl. Phys.*

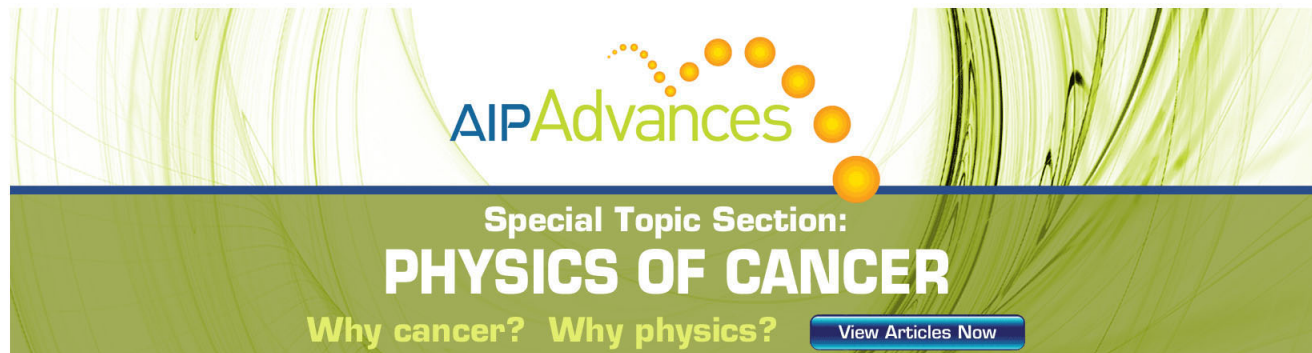
Journal Homepage: <http://jap.aip.org/>

Journal Information: http://jap.aip.org/about/about_the_journal

Top downloads: http://jap.aip.org/features/most_downloaded

Information for Authors: <http://jap.aip.org/authors>

ADVERTISEMENT

The advertisement features a green background with abstract, flowing lines. At the top, the 'AIP Advances' logo is displayed, with 'AIP' in blue and 'Advances' in green, accompanied by a series of orange dots. Below the logo, the text 'Special Topic Section: PHYSICS OF CANCER' is written in white, with 'PHYSICS OF CANCER' in a larger, bold font. At the bottom, the phrase 'Why cancer? Why physics?' is written in yellow, and a blue button with the text 'View Articles Now' is located on the right side.

AIP Advances

Special Topic Section:
PHYSICS OF CANCER

Why cancer? Why physics? [View Articles Now](#)

rf magnetron sputter deposition of transparent conducting Nb-doped TiO₂ films on SrTiO₃

Meagen A. Gillispie

Iowa State University, Ames, Iowa 50011

Maikel F. A. M. van Hest,^{a)} Matthew S. Dabney, John D. Perkins, and David S. Ginley

National Renewable Energy Laboratory, Golden, Colorado 80401

(Received 31 August 2006; accepted 8 December 2006; published online 14 February 2007)

rf magnetron sputtering, an established and scalable large area deposition process, is used to deposit Nb:TiO₂ and Ta:TiO₂ films onto (100) SrTiO₃ substrates at temperatures T_S ranging from room temperature to 400 °C. Optical, electrical, and structural properties similar to those reported for pulsed laser deposition grown films were obtained. In particular, the most conducting Ti_{0.85}Nb_{0.15}O₂ films, grown at $T_S \approx 375$ °C, are epitaxially oriented anatase films with conductivity of 3000 S cm⁻¹, carrier concentration of 2.4×10^{21} cm⁻³, Hall mobility of 7.6 cm² V⁻¹ s⁻¹, and optical transparency $T > 80\%$ from 400 to 900 nm. The conductivity is strongly correlated with the intensity of the anatase (004) x-ray diffraction peak. © 2007 American Institute of Physics.

[DOI: 10.1063/1.2434005]

I. INTRODUCTION

Flat panel displays, light emitting diodes, and solar cells all require the use of transparent contacts typically employing transparent conducting oxides (TCOs).^{1–5} Sn-doped In₂O₃ (ITO) is commonly the TCO of choice because of its high conductivity, transparency, and ease of deposition of very thin films.^{6–8} However, ITO has significant drawbacks, namely, it is difficult to pattern and needs processing at elevated temperatures to get optimum performance as well as requires indium which is increasingly expensive. Hence, there is increasing interest in finding suitable In-free alternatives to ITO for TCO applications. At present, both doped SnO₂ and ZnO find use in windows, flat panel displays, and solar cells.² However, both have significant drawbacks including high deposition temperatures and chemical instability, respectively.^{2,9,10}

Recently, Nb- and Ta-doped anatase TiO₂ films have been identified as potential TCO materials.^{11–13} The anatase polymorph of TiO₂ (*I*₄/amd) has long been used as a photocatalyst,¹⁴ yet has only recently gained attention for its favorable electronic properties (energy gap $E_g = 3.2$ eV, effective mass $m^* \sim 1m_e$),¹⁵ which indicate that it might be suitable for TCO applications. In addition to potential technology applications, anatase TiO₂ as a TCO is fundamentally interesting because its conductivity is due to *d* electrons¹² rather than *s* electrons like other TCOs.^{10,16} Possible donor dopants for Ti include the 5+ cations V, Nb, and Ta. Thin, 40 nm thick, transparent Nb-doped anatase TiO₂ films grown on strontium titanate (SrTiO₃, STO) by pulsed laser deposition (PLD) have demonstrated conductivities σ on the order of $(2-4) \times 10^3$ S cm⁻¹ and Hall mobilities $\mu_H = 15-22$ cm² V⁻¹ s⁻¹ at dopant concentrations of 3–6 mol %.^{11,12,17} Somewhat surprisingly, conductivity remained on the order of 10^3 S cm⁻¹ for dopant concentrations as high as 20 mol %, although transparency decreased sig-

nificantly with the higher doping levels. PLD grown Ta-doped TiO₂ films on STO were found to have similar electrical properties for Ta dopant concentration up to 15 mol %.¹³

In this paper, it is demonstrated that TCO films with performance similar to that for PLD films^{11–13} can be made by radio-frequency (rf) magnetron sputter deposition from both Nb- and Ta-doped TiO₂ targets. For technology applications, the use of low-cost, large area, sputtering techniques to fabricate TCO films is preferable to more expensive means such as PLD. We present the structural, electrical, and optical properties of sputtered Nb and Ta-doped TiO₂ films deposited on STO at temperatures from room temperature up to ~ 400 °C. Optimized sputtered Ti_{0.85}Nb_{0.15}O₂ films had $\sigma \sim 2000-3000$ S cm⁻¹ with $\mu_H \sim 7-8$ cm² V⁻¹ s⁻¹ while Ti_{0.8}Ta_{0.2}O₂ films had $\sigma \sim 300$ S cm⁻¹ with $\mu_H \sim 0.4$ cm² V⁻¹ s⁻¹. Furthermore, a strong correlation is observed between the electrical conductivity and simple measures of the anatase phase crystallinity.

II. EXPERIMENT

Nb- and Ta-doped TiO₂ films were sputter deposited onto 5×10 mm² polished STO (100) substrates (MTI Crystal) using a 2 in. oxide target consisting of 7.5 mol % Nb₂O₃ in TiO₂ (Ti_{0.85}Nb_{0.15}O₂, 99.9%, Plasmaterials) and 10 mol % Ta₂O₅ in TiO₂ (Ti_{0.8}Ta_{0.2}O₂, 99.95%, Plasmaterials), respectively. The substrates were secured to a 2×2 in.² piece of Corning 1737 glass using silver epoxy for mounting in the substrate holder. A 2 in. sputtering gun (Angstrom Sciences Onyx 2 magnetron sputter source) was positioned at a 45° angle to the substrate holder that had a resistive heater capable of temperatures up to 900 °C. The target to substrate distance is 8 cm at the center of the target and substrate. For films deposited from a single target, this configuration results in a lateral thickness gradient. However, the thickness variation across a single STO substrate is only $\sim 7\%$, and hence was ignored for the analysis presented here. Films were deposited in pure argon (grade 5.0) at a flow rate of 20 sccm

^{a)}Electronic mail: maikel_van_hest@nrel.gov

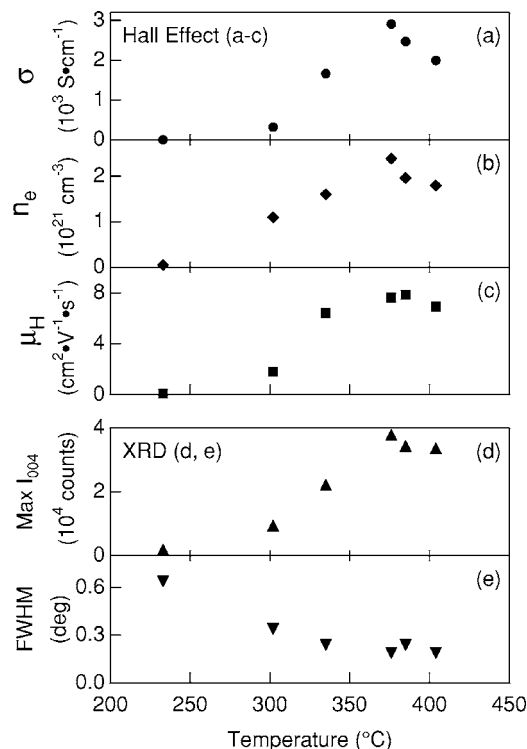


FIG. 1. Electrical and structural properties of Nb-doped TiO₂ films (15 mol %) deposited on STO at various temperatures: (a) conductivity σ , (b) carrier concentration n_e , and (c) Hall mobility μ_H . (d) Maximum intensity of anatase (004) XRD peak and (e) FWHM of anatase (004) XRD peak.

and a system pressure of 4.5 mTorr (SCCM denotes cubic centimeter per minute at STP). Temperatures ranged from room temperature to heater block temperature of 550 °C, corresponding to a maximum front surface substrate temperature T_S of 404 °C as measured with a thermocouple. A rf-sputtering power (Manitou series PB-3 rf power system) of 25–30 W was required to attain films with thickness of approximately 200 nm on the center of the STO substrate after 1 h of deposition. The structure of the films was analyzed using x-ray diffraction (XRD) with a two-dimensional detector (Bruker D8 Discover). Electrical properties were measured using a BioRad Hall probe system. Optical transmission and reflection were analyzed over the wavelength range of 400–1600 nm using a combination of UV, visible, and near infrared (NIR) light sources and detectors.¹⁸

III. RESULTS AND DISCUSSION

Conductivity, carrier concentration, and Hall mobility of the Nb-doped TiO₂ (Ti_{0.85}Nb_{0.15}O₂) films on STO as a function of deposition temperature are shown in Figs. 1(a)–1(c), respectively. Films deposited at temperatures above 300 °C had conductivity higher than 1500 S cm⁻¹. Conductivity reached a maximum value of 3000 S cm⁻¹ for films deposited at $T_S \sim 375$ °C and remained above 2000 S cm⁻¹ for T_S up to 400 °C. Both mobility [Fig. 1(c)] and carrier concentration [n_e , Fig. 1(b)] followed the same general trend as conductivity. The film deposited at 375 °C had $n_e = 2.4 \times 10^{21} \text{ cm}^{-3}$ and $\mu_H = 7.6 \text{ cm}^2 \text{ V}^{-1} \text{ s}^{-1}$, which agree quite well with the results for films of similar composition grown at about 550 °C on STO using PLD.^{11,12} Ta-doped TiO₂

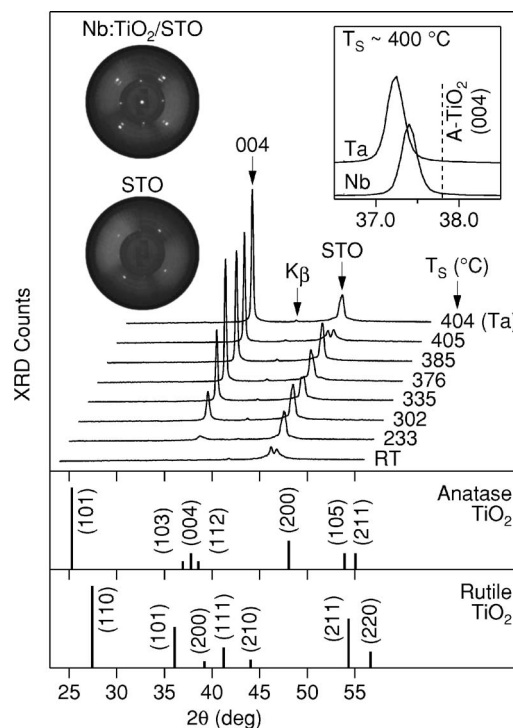


FIG. 2. Top: XRD 2θ spectra of Nb-doped TiO₂ (Ti_{0.85}Nb_{0.15}O₂) and Ta-doped TiO₂ (Ti_{0.8}Ta_{0.2}O₂) on STO at varying deposition temperatures. Middle: Anatase TiO₂ x-ray powder diffraction pattern (JCPDS 21-1272). Bottom: Rutile TiO₂ x-ray powder diffraction pattern (JCPDS 21-1276). Insets: Pole figures taken at 2θ = 37° ± 1° for a bare STO substrate (lower) and for a TiO₂ film on STO (upper). Upper right inset: 2θ spectra for Ta- and Nb-doped TiO₂ on STO for films grown at ~400 °C.

(Ti_{0.8}Ta_{0.2}O₂) films were also sputter deposited on STO at 404 °C. For these Ta-doped films, $\sigma = 300 \text{ S cm}^{-1}$ with $n_e \sim 5 \times 10^{21} \text{ cm}^{-3}$, about twice that measured for the best Nb-doped TiO₂ film, and $\mu_H < 1 \text{ cm}^2 \text{ V}^{-1} \text{ s}^{-1}$, at least ten times lower. For the Ti_{1-x}Ta_xO₂ films grown by PLD on STO at 550 °C, the maximum conductivity occurred for $x = 0.05$ where $\sigma = 4000 \text{ S cm}^{-1}$ with $n_e = 1.4 \times 10^{21} \text{ cm}^{-3}$ and $\mu_H = 18 \text{ cm}^2 \text{ V}^{-1} \text{ s}^{-1}$ with a general increase in n_e with dopant concentration and a monotonic suppression of μ_H at higher doping levels.¹³ For the sputter-deposited Ta-doped films, the Ta content, $x = 0.2$, is four times higher and the carrier concentration is 3.6 times higher, consistent with nearly linear substitutional doping, but the mobility, $\sim 1 \text{ cm}^2 \text{ V}^{-1} \text{ s}^{-1}$, is markedly less, suggesting that these sputtered Ta-doped films are likely overdoped.

The main panel of Fig. 2 shows 2θ spectra for Nb-doped TiO₂ films grown on (100) STO at temperatures from room temperature to 405 °C as well as one spectrum for a Ta-doped TiO₂ film grown at 404 °C. For all spectra, three features are observed as indicated by the labeled arrows. The STO (200) peak, expected at 46.5°, appears but with suppressed intensity or even split into a doublet due to detector saturation and a weak peak observed in all the spectra at 41.85° is due to K_β STO (200) diffraction. No additional features are observed for the room temperature deposited Nb-doped film. For all the films deposited at higher temperatures, an additional single peak is observed at 2θ ≈ 37.5°. This peak generally increases in intensity with increasing substrate temperature and, for the Nb-doped films, shifts

monotonically from $2\theta=37.75^\circ$ at $T_s=233^\circ\text{C}$ to $2\theta=37.4^\circ$ at $T_s=376^\circ\text{C}$, the substrate temperature for the most conducting films. The bottom two panels show the expected powder diffraction patterns for anatase and rutile TiO_2 . No line from the expected rutile pattern can explain the observed diffraction, but based on only the 2θ position of the single film peak observed, one cannot definitively distinguish between the anatase (103) and (004) peaks. Considering symmetry, (004) oriented anatase is expected for anatase TiO_2 on (100) STO and this is confirmed by the two pole figures taken at $2\theta=37\pm1^\circ$ included as insets. For the bare STO substrate pole figure, four spots 90° apart in ϕ are observed at $\chi=55^\circ$, corresponding to the STO (111) expected at $2\theta=40^\circ$ but which is observed in this pole figure due to poor 2θ resolution in the pole figure measurements. In the Nb: TiO_2 /STO pole figure these same four STO spots are observed with additional fourfold symmetric film spots at $\chi=60^\circ$ and 40° as well as a center film spot at $\chi=0^\circ$. This is exactly as expected for epitaxial (004) oriented anatase TiO_2 on (100) STO with the observed film spots corresponding to anatase (112), (103), and (004) diffractions, respectively. Figure 2 also includes the XRD spectrum for a Ta-doped TiO_2 film deposited at 404°C . Like with Nb-doped TiO_2 and PLD Ta-doped TiO_2 ,¹³ the sputter-deposited Ta-doped TiO_2 film crystallized in (004) oriented anatase but with the (004) diffraction at $2\theta=37.25^\circ$ vs 37.4° for Nb-doped TiO_2 as shown in Fig. 2 inset. Note that the (004) diffraction peak for both the Nb- and Ta-doped TiO_2 occurs at lower 2θ corresponding to a larger lattice constant than for undoped anatase TiO_2 .

The intensity of the (004) anatase peak increases significantly as deposition temperature was raised from 233 to 375 $^\circ\text{C}$, as seen in Fig. 1(d). Comparing the conductivity data shown in Fig. 1(a) with XRD data shown in Fig. 1(d), it is clear that conductivity is strongly correlated with the anatase crystallinity including even the small conductivity decrease observed at the highest two substrate temperatures. At higher substrate temperatures, a crossover from anatase to rutile structure is expected.¹⁹ Full width at half maximum (FWHM) of the (004) peak is also shown in Fig. 1(e). FWHM decreased as (004) intensity increased, and above 375 $^\circ\text{C}$ peak intensity and FWHM appear to have saturated, showing that the films are fully crystalline.

Optical transmission and reflection spectra of selected Nb-doped TiO_2 samples are shown in Fig. 3 with the transmission spectra normalized to a bare STO substrate. In general, all films were greater than $\sim 80\%$ transparent through the visible portion of the electromagnetic spectrum (400–700 nm). The film with the highest conductivity ($T_s=375^\circ\text{C}$) had the lowest transmission, particularly in the infrared. For this film, the broad decrease in the transmission is also accompanied by an increase in reflection as wavelength increases. This is as expected for plasma oscillations of the free conduction band electrons (Drude model) rather than for a $d-d$ absorption, which could cause coloration due to partially filled d bands. In the Drude model, the crossover from transparent to reflecting with increasing wavelength occurs at the plasma wavelength given by

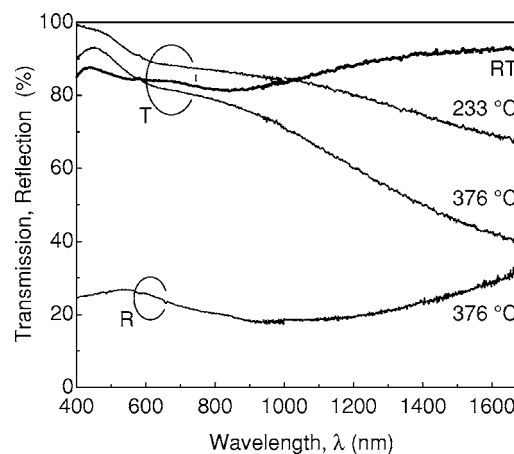


FIG. 3. Optical transmission and reflection spectra for Nb-doped TiO_2 samples grown at different substrate temperatures as labeled. The transmission spectra are normalized vs a bare substrate.

$$\lambda_p = 2\pi c \sqrt{\frac{\epsilon_\infty m^*}{4\pi N e^2}}, \quad (1)$$

where c is the speed of light, ϵ_∞ the dielectric function in the visible, m^* the electron effective mass, N the free electron density, and e the electron charge.¹⁸ Taking $\epsilon_\infty=6.25$ and $m^*=1m_e$ as appropriate for anatase TiO_2 ,²⁰ $N=2.4 \times 10^{21} \text{ cm}^{-3}$ as measured here for the film deposited at 376 $^\circ\text{C}$, gives $\lambda_p=1700 \text{ nm}$, very consistent with the spectra shown in Fig. 3.

Overall, the transparency of these sputtered films is lower than that reported by Furubayashi *et al.* for PLD films of the same composition (transmittance $>85\%$).^{11,12} This is likely due to differences in thickness. All the sputtered films analyzed here were $\sim 200 \text{ nm}$ thick, while the PLD films by Furubayashi *et al.* were 40 nm thick. Note that the surface roughness of sputtered films was found to be $\sim 2 \text{ nm}$ [atomic force microscopy (AFM)].

Recent publications^{21,22} suggested that the high conductivity observed for Nb-doped anatase TiO_2 films grown on STO substrates might be due to Nb diffusion into the STO substrate rather than to conductivity of the Nb-doped TiO_2 film itself. In this present work, 200 nm thick anatase $\text{Ti}_{0.85}\text{Nb}_{0.15}\text{O}_2$ films grown at $\sim 400^\circ\text{C}$ have a maximum conductivity of $\sigma \sim 3000 \text{ S cm}^{-1}$, the same as for 40 nm thick films of the same composition grown by PLD.¹² Since conductivity is an intrinsic material property independent of film thickness, this strongly suggests that the observed conductivity is due to the conductivity of the Nb-doped TiO_2 film itself and not due to Nb diffusion into the STO substrate. In addition, as shown in Fig. 1(a), for the Nb-doped TiO_2 films deposited by sputtering, the maximum conductivity occurs at a substrate temperature of 376 $^\circ\text{C}$ and the conductivity actually decreases for higher substrate temperatures. This again suggests that the conductivity is not due to Nb diffusion into the substrate. In fact, the occurrence of the maximum conductivity at 376 $^\circ\text{C}$ is correlated with maximum anatase (004) XRD intensity at the same temperature. Last, the consistency of the observed IR features in the optical spectra with the Drude model as applied to doped anatase TiO_2 and the observation of similar conductivities for Ta-

doped anatase TiO₂ films further support the conclusion that the observed conductivity comes from substitutional doping of the TiO₂ film itself.

IV. CONCLUSIONS

In summary, highly conductive Nb-doped anatase TiO₂ films were deposited on STO using rf magnetron sputtering. Films doped with 15 mol % Nb exhibited similar performance characteristics as PLD grown films. Conductivity was found to be well correlated with simple measures of anatase phase crystallinity. Taken collectively, these results on sputtered films along with those for PLD films¹² clearly show that substitutionally doped anatase TiO₂ thin films are viable for use as transparent conductors.

ACKNOWLEDGMENT

This work was supported by the Laboratory Discretionary Research and Development (LDRD) program at the National Renewable Energy Laboratory (NREL).

¹D. S. Ginley and C. Bright, MRS Bull. **25**, 15 (2000).

²R. G. Gordon, MRS Bull. **25**, 52 (2000).

³G. Haacke, Annu. Rev. Mater. Sci. **7**, 73 (1977).

⁴H. Hosono, H. Ohta, M. Orita, K. Ueda, and M. Hirano, Vacuum **66**, 419

(2002).

⁵H. Kawazoe, H. Yanagi, K. Ueda, and H. Hosono, MRS Bull. **25**, 28 (2000).

⁶B. G. Lewis and D. C. Paine, MRS Bull. **25**, 22 (2000).

⁷O. N. Mryasov and A. J. Freeman, Phys. Rev. B **64**, 233111 (2001).

⁸R. B. H. Tahar, T. Ban, Y. Ohya, and Y. Takahashi, J. Appl. Phys. **83**, 2631 (1998).

⁹C. M. Dai, C. S. Su, and D. S. Chuu, Appl. Phys. Lett. **57**, 1879 (1990).

¹⁰T. Minami, MRS Bull. **25**, 38 (2000).

¹¹Y. Furubayashi, T. Hitosugi, Y. Yamamoto, Y. Hirose, G. Kinoda, K. Inaba, T. Shimada, and T. Hasegawa, Thin Solid Films **496**, 157 (2006).

¹²Y. Furubayashi, T. Hitosugi, Y. Yamamoto, K. Inaba, G. Kinoda, Y. Hirose, T. Shimada, and T. Hasegawa, Appl. Phys. Lett. **86**, 252101 (2005).

¹³T. Hitosugi *et al.*, Jpn. J. Appl. Phys., Part 2 **44**, L1063 (2005).

¹⁴A. Fujishima and K. Honda, Nature (London) **238**, 37 (1972).

¹⁵H. Tang, K. Prasad, R. Sanjinys, P. E. Schmid, and F. Lvy, J. Appl. Phys. **75**, 2042 (1994).

¹⁶A. J. Freeman, K. R. Poeppelmeier, T. O. Mason, R. P. H. Chang, and T. J. Marks, MRS Bull. **25**, 45 (2000).

¹⁷M. S. Dabney, M. F. A. M. van Hest, M. A. Gillispie, J. D. Perkins, and D. S. Ginley, Thin Solid Films Thin Solid Films (to be published).

¹⁸J. D. Perkins *et al.*, Appl. Surf. Sci. **223**, 124 (2004).

¹⁹N. Martin, C. Rousselot, D. Rondot, F. Palmirino, and M. Rene, Thin Solid Films **300**, 113 (1997).

²⁰H. Tang, H. Berger, P. E. Schmid, and F. Lvy, Solid State Commun. **92**, 267 (1994).

²¹Y. Furubayashi, T. Hitosugi, and T. Hasegawa, Appl. Phys. Lett. **88**, 226103 (2006).

²²Q. Wan and T. H. Wang, Appl. Phys. Lett. **88**, 226102 (2006).